IEEE Access
Multidisciplinary ⋮ Rapid Review ⋮ Open Access Journal

Received August 11, 2020, accepted August 24, 2020, date of publication August 31, 2020, date of current version September 11, 2020.

Digital Object Identifier 10.1109/ACCESS.2020.3019822

A Wideband Folded Reflectarray Antenna Based on Single-Layered Polarization Rotating Metasurface

WEI SU[1,2,3], (Member, IEEE), WENHAO LUO[3], ZHENHUA NIE[3], WEN-WEN LIU[4], ZHEN-HUA CAO[4], AND ZHI WANG[4]

[1]MOE Key Laboratory of Disaster Forecast and Control in Engineering, Guangzhou 510632, China
[2]Science and Technology on Reliability Physics and Application Technology of Electronic Component Laboratory, China Electronic Product Reliability, and Environmental Testing Research Institute, Guangzhou 510610, China
[3]School of Mechanics and Construction Engineering, Jinan University, Guangzhou 510632, China
[4]School of Mechanics and Safety Engineering, Zhengzhou University, Zhengzhou 450001, China

Corresponding author: Wei Su (suwei5@126.com)

ABSTRACT A wideband folded reflectarray antenna (FRA) based on single-layered polarization rotating metasurface (PRM) is proposed. The FRA is composed of a wideband polarization grid (PG), a wideband PRM and a wideband circular waveguide as the primary source. First, a wideband polarization rotating unit cell consisting of rhombus-shaped metal patch etched on dielectric substrate is designed, which can be used to rotate polarization of the reflective wave 90° relative to that of the incident wave. The element and its mirror image can provide 0°, 90°, 180° and 270° phase shifts with 2-bit phase quantization and relatively higher polarization conversion rates in the Ku band. Due to the introduction of PG and PRM, the distance between the PG surface and the feed phase center can be reduced to about 1/2 of the distance between the imaginary feed and PRM reflectarray. Finally, a wideband FRA consisting of 315 elements with circular aperture is designed, fabricated and measured. The measured results indicate that the proposed antenna achieves 39.5% 3-dB gain bandwidth with 25.5 dBi peak gain at 15 GHz. Its maximum aperture efficiency is about 40%. Low-profile and wideband features of the FRA make it be a candidate in the wireless communication systems.

INDEX TERMS Folded, reflectarray, polarization rotating reflection surface (PRRS), polarization grid.

I. INTRODUCTION

High-gain antennas have been playing an extremely significant role in many fields such as satellite communications, radar detection and radio astronomy. Traditional high-gain antennas mainly include parabolic antennas and large array antennas. Although the parabolic antennas have several advantages such as high gains and broad bands, they are not easily transported and installed, because of their bulky sizes. The parabolic surfaces also need high processing accuracies, resulting in high costs. Moreover, the large array antennas need complex feeding networks generally, which leads to lower radiation efficiencies. As a new type of high gain antennas combined with the parabolic antenna and the antenna array, the reflectarray antenna has attracted much attention over years. Compared with the parabolic antenna and the array antenna, the reflectarray antenna has prominent advantages such as planar structure, light weight, easy fabrication, low cost, and easy to realize flexible beam scanning. In addition, due to its space feeding, the reflectarray antenna could avoid extra losses of the feeding network and improve the antenna efficiencies [1]–[3].

Recently, the reflectarray antennas have been made great progress in their performance improvements such as wide bands, multiple polarizations and high gains. However, their profiles are much higher, which limit their application areas. In order to reduce profiles of the reflectarray antennas, the folded reflectarray antennas (FRAs) were proposed in [4]–[6]. This kind of low-profile reflectarrays mainly consists of a planar reflectarray, a feed located at the bottom-layer reflectarray center, and an upper-layer PG. The lower planar reflectarray transforms the spherical plane wave into the planar wave, and twists the polarization, while the upper polarization grid realizes the polarization transmission and

The associate editor coordinating the review of this manuscript and approving it for publication was Weiren Zhu.

reflection. Many kinds of high-performance FRAs, such as high-gain, high-efficiency, beam-shaped and beam-scanned FRAs, have been proposed in [8]–[19]. However, it is generally known that the reflectarray antenna has the inherent defect of narrow band, which seriously restricts their application areas. To address this problem, many new approaches for broadening bandwidths of the FRA are proposed. Two kinds of broadband FRAs are proposed in [16] and [17], which achieves 16% and 30% 1-dB gain bandwidth, respectively. Although the bandwidths of FRA in these two papers have been improved, the element of these two FRAs contains double-layer substrates or single-layer substrate and air, respectively, which increases the assembly difficulty and the processing cost. Therefore, it is important to design a new wideband FRA with simple design and lower cost.

Different from the wideband FRA in [16] and [17], the proposed FRA is designed by using a novel polarization rotating element with 2-bit phase quantitation for the first time, which greatly simplifies the design process. Moreover, the PRM reflectarray contains only single-layer substrate and metal patch and leads to reduce the cost of the proposed FRA. Finally, by using the wideband 2-bit polarization rotating element, the proposed FRA obtains wider bandwidth and higher aperture efficiency.

II. PRINCIPLE OF THE FRA

Conventional reflectarray antenna consists of a feed and a planar reflective array, as shown in the Figure7 (a). Illuminated by the spherical wave from the feed, the reflectarray radiates the plane wave into the free space. However, large focal-diameter ratio (F/D) of the reflectarray increases its volume, which restricts their application areas. Figure 1 presents the basic schematic diagram of the proposed FRA. The FRA consists of a bottom-layer planar PRM reflectarray, a top-layer PG and a feed (wideband circular waveguide). The PRM reflectarray can be used to rotate polarization of the reflective wave 90° relative to that of the incident wave with providing phase-shifting compensation. The PG is a polarization selective surface, which can transmit one LP wave while fully reflect its orthogonal LP wave. The spherical LP wave (green solid line corresponding to y-polarization wave) emitted by the feed is first reflected by the PG, and then reflected with 90° polarization twist by the PRM reflectarray at the same time, providing phase-shifting compensation, producing its orthogonal LP wave (red solid line corresponding to x-polarization wave). This high gain LP wave passes through the top PG and radiates into the free space. The equivalent feed position of the FRA coincides with the feed position of the traditional reflectarray antenna. As shown in Figure 1, based on the ray tracing principle, height of the proposed antenna is about 1/2 of the distance between the imaginary feed and PRM reflectarray.

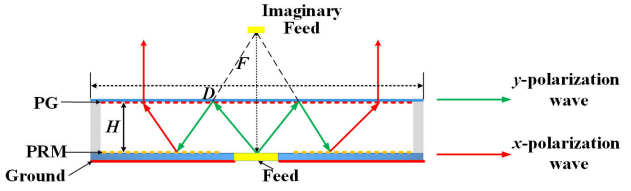

FIGURE 1. Diagram of the proposed FRA.

III. ELEMENT DESIGN

Configurations of the proposed PRM reflectarray element and the PG unit are illustrated in Fig. 2. The PRM reflectarray element consists of a rhombus-shaped metal patch etched on dielectric substrate with height H = 2 mm and relative permittivity 2.2, which rotates polarization of the reflective wave 90° relative to that of the incident wave. Compared with the traditional elements in [15] and [16], the proposed PRM reflectarray element contains only one substrate, which greatly simplifies the design difficulties. The PG unit consists of one substrate layer and one metal layers. The metal strip is etched on one side of the substrate with the same relative permittivity 2.2 and thickness H = 2 mm. Detailed parameter values of these two structures are given in Table 1. In addition, the electromagnetic performance of this element is analyzed by Ansys HFSS software under Floquet periodic boundary conditions.

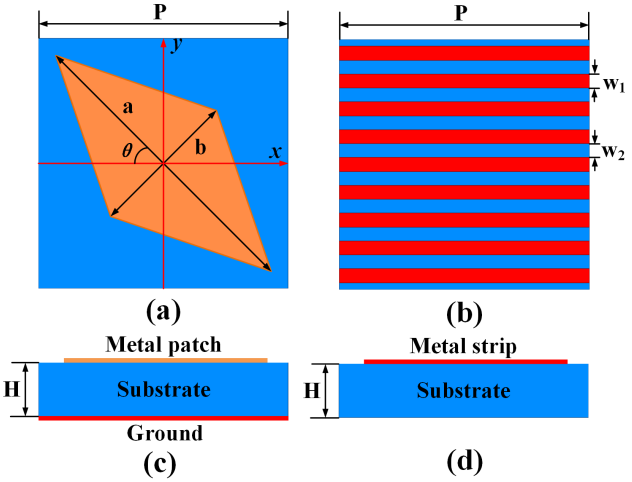

FIGURE 2. Configurations of the PRM reflectarray element and the PG unit. (a) the PRM reflectarray element with $\theta = 45°$, (b) the PG unit, (c) side view of the PRM element (d) side view of the PG element.

TABLE 1. Key Parameters of the PRM reflectarray element and the PG unit.

Parameters	P	a	b	a_1	b_1	H	w_1	w_2
Value (mm)	9	5.5	2.7	1.7	3.1	2	0.5	0.5

The operating principle of the PRM reflectarray element is shown in the Fig. 3. As shown in Fig. 3 (a), the incident wave E^i can be decomposed into two orthogonal components with equal amplitude and phase. By adjusting the element

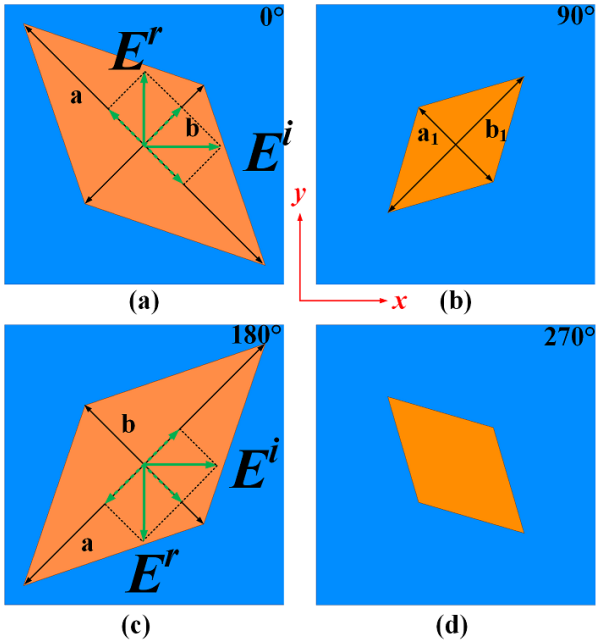

FIGURE 3. Two 2-bit phase quantization elements (a) 0° phase shift case, (b) 90° phase shift case, (c) 180° phase shift case, (d) 270° phase shift case.

dimensions a and b in two orthogonal directions properly, the polarization of the reflective wave E^r is converted by 90° compared with the incident wave E^i. The operating principle for the 180° phase shift case is similar to that for the 0° phase shift case. As shown in Fig. 3 (c), since the patch is rotated by 90° in thr clockwise direction compared with the patch in the Figure3 (a), the reflective wave E^r pints to opposite direction, and then a 180° phase difference is produced. By adjusting the element dimensions a and b, the element finally obtains 0°, 90°, 180° and 270° phase shift cases as shown in the Fig. 3 (a), (b), (c) and (d).

Simulated reflective magnitude and phases versus frequency for the element with the 0°, 90°, 180° and 270° phase shift cases are presented in Fig. 4. As shown in the figure, its

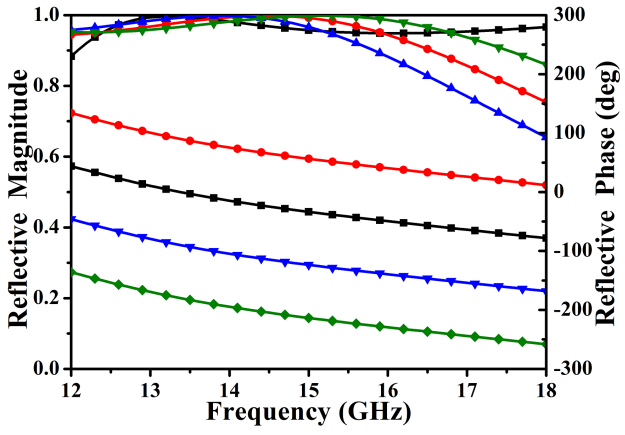

FIGURE 4. Simulated reflective magnitude and phases versus frequency for the PRM element with the 0°, 90°, 180° and 270° phase shift cases.

reflective magnitude amplitudes at 12–17 GHz are more than 0.8, reflective phase shows that the similar phase difference, about 90°, are achieved at 12-18 GHz between each two adjacent curves.

Since the majority of the elements are obliquely illuminated by the feed, it is worthy of studying the reflective performance of the element with different incident angles. Fig. 5 presents the simulated reflective magnitude and phases versus frequency with different incident angles. Obviously, almost no significant changes are observed, which is beneficial for designing the FRA. Therefore, the proposed FRA is designed based on the reflective phases under normal incidence.

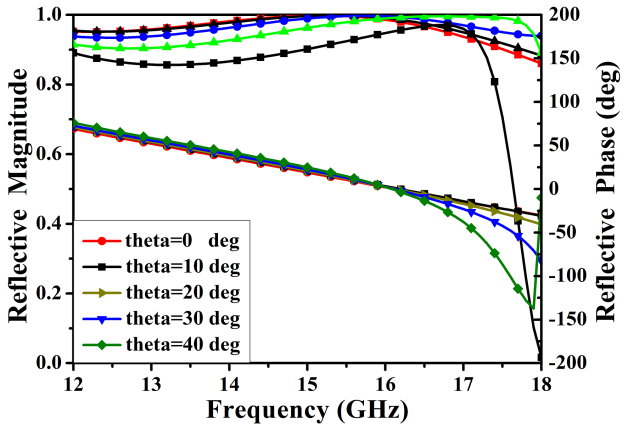

FIGURE 5. Simulated reflective magnitude and phases versus frequency with different incident angles.

Simulated transmission magnitudes of two polarization waves (x-polarization and y-polarization) versus frequency for the PG element with different incident angles are presented in Fig. 6. As shown in the figure, the PG element has higher polarization selection ratios, which are greater than 90% in the operating band. Almost all the y-polarized waves

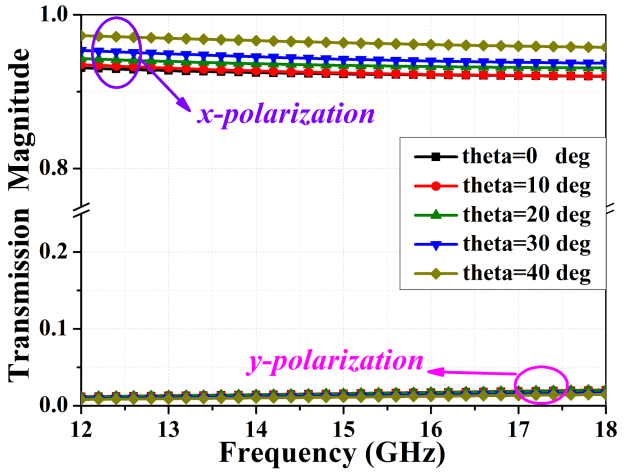

FIGURE 6. Simulated transmission magnitudes of two polarization waves (x-polarization and y-polarization) versus frequency for the PG element with different incident angles.

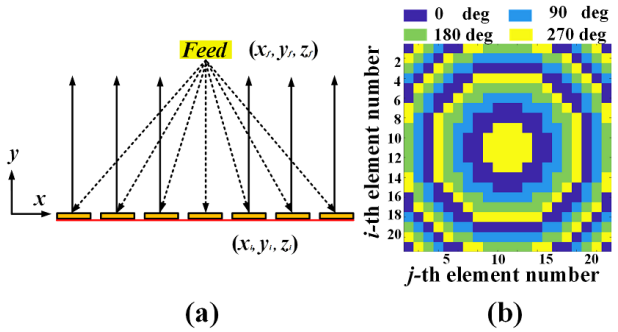

FIGURE 7. Phase compensation of the traditional planar reflectarray. (a) Principle diagram of the phase compensation, and (b) phase distribution of the planar reflectarray.

are transmitted converted while all the x-polarized waves are reflected, which meets the design requirements.

Based on the aforementioned results, we conclude that the PRM reflectarray element can rotate one LP polarization wave to its orthogonal LP wave, and provide enough phase shifts to achieve high gain. The PG element can almost completely transmit one LP polarization while reflect its orthogonal LP wave. These features will play a significant role in the array design.

IV. DESIGN OF THE REFLECTARRAY ANTENNA AND ITS PERFORMANCE

A. PHASE DISTRIBUTION OF THE REFLECTARRAY

Sketch of the reflectarray is shown in Fig. 7(a). To achieve a high gain beam collimation, the required compensation phase for the (i, j)-th element in the reflectarray can be expressed as

$$\varphi_{unit}\left(x_i, y_j\right) = \varphi_0 - \varphi_{feed}\left(x_i, y_j\right) \tag{1}$$

where (x_i, y_j) is the coordinate position of the (i, j)-th element in the reflectarray, φ_0 is a constant phase, φ_{feed} represents the incident wave phase, which is denoted by

$$\varphi_{feed}\left(x_i, y_j\right) = -2\pi\frac{d_{i,j}}{\lambda} \tag{2}$$

$d_{i,j}$ stands for the distance between the feed phase center and point (x_i, y_j), and λ represents the wavelength in free space. Owing to the 2-bit phase quantization provided by the element, traditional continuous reflective phase distribution can be replaced by the discrete phase distribution. The 2-bit discrete phase for the (i, j)-th element in the reflectarray can be determined by

$$\varphi_d\left(x_i, y_j\right) = \begin{cases} 0^\circ, & 0^\circ \le \varphi_{unit}\left(x_i, y_j\right) < 90^\circ \\ 90^\circ, & 90^\circ \le \varphi_{unit}\left(x_i, y_j\right) < 180^\circ \\ 180^\circ, & 180^\circ \le \varphi_{unit}\left(x_i, y_j\right) < 270^\circ \\ 270^\circ, & 270^\circ \le \varphi_{unit}\left(x_i, y_j\right) < 360^\circ \end{cases} \tag{3}$$

According to Equation (3), the 2-bit reflective phase distribution of the reflectarray is calculated, as shown in Fig. 7(b).

B. FEED DESIGN

A standard LP circular waveguide is chosen as the feed, as shown in Fig. 8. Its photograph, measured $|S_{11}|$ and radiation patterns at the center frequency 15 GHz are presented in Figs. 8(a) and 8(b). Its operating frequency band is 12-18 GHz, which covers the required frequency band of the FRA. The -10 dB beamwidths of the E-plane and H-plane patterns are $\pm 60.1^\circ$ and $\pm 60.2^\circ$, respectively. Obviously, there is a good consistency between the E-plane and H-plane patterns in the feed illumination angular domain. The E-plane and H-plane patterns of the feed are approximately expressed as $\cos^5\theta$. The whole reflectarray antenna is analyzed by the full-wave software Ansys HFSS.

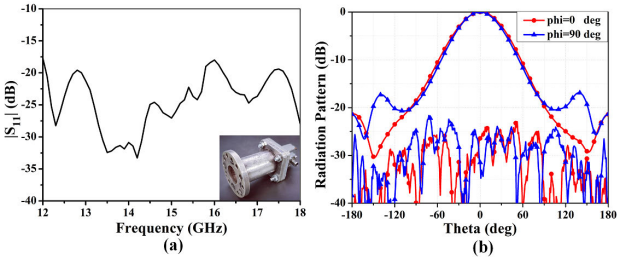

FIGURE 8. The standard LP circular waveguide. (a) Photograph of the feed and measured $|S_{11}|$. (b) measured patterns of the feed in the xoz-plane and yoz-plane at 15 GHz.

C. ARRAY DESIGN

Based on the design principle and above analyses, the wideband FRA at the center frequency 15 GHz is designed and simulated by using ANSYS HFSS software. The lower PRM reflectarray has a circular aperture with 189 mm ($9.45\lambda_0$, λ_0 is the wavelength at 15 GHz) diameter and 315 elements. The F/D value of the FRA is 0.5. The upper PG has the same aperture as the lower PRM reflectarray. The distance between the lower PRM reflectarray and the upper PG is 45 mm (about F/2). The feed is located at the center of the bottom-layer PRM refelctarray. Some dielectric screws are used to fasten and separate two planar arrays. In order to validate the design, the proposed FRA is fabricated, and its radiation patterns are tested by a far-field measurement system in an anechoic chamber. Photograph of the proposed FRA is shown in Fig. 9.

Simulated and measured normalized radiation patterns of the proposed FRA at different frequencies are presented in Fig. 10. As shown in the figure, the measured radiation patterns agree well with the simulated ones. At the center frequency 15 GHz, the measured E-plane and H-plane half-power beamwidths are 7.1° and 7.2°, respectively. The measured cross-polarization levels in the maximum radiation direction are less than -20 dB, and the measured sidelobe levels are less than -20 dB. Measured results indicate that the FRA has stable radiation patterns in the whole operating bands. Fig. 11 presents the measured results ($|S_{11}|$ and gain) for the antenna. As shown in the figure, the FRA has 40% -10 dB reflection coefficient bandwidth and 39.5% 3-dB

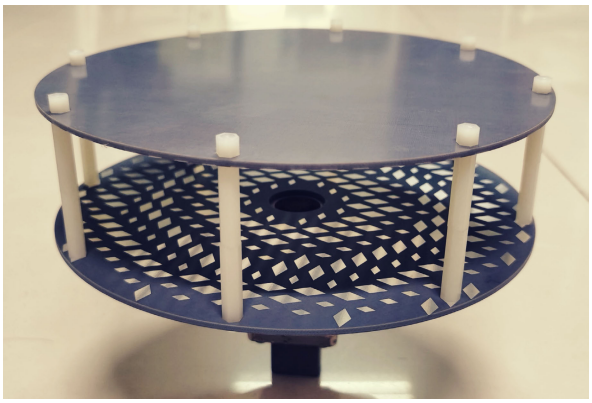

FIGURE 9. Photograph of the proposed FRA.

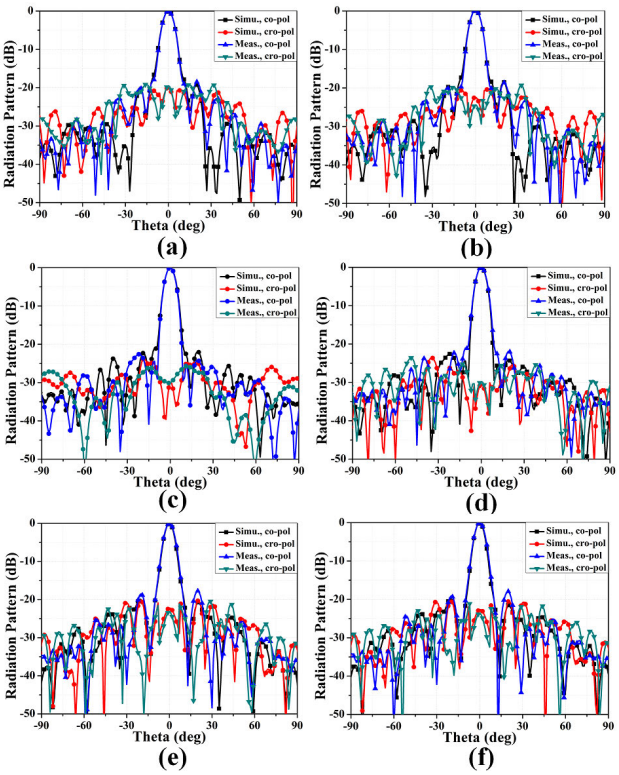

FIGURE 10. Simulated and measured normalized radiation patterns of the proposed FRA in (a) the xoz plane at 13 GHz, (b) the yoz plane at 13 GHz, (c) the xoz plane at 15 GHz, (d) the yoz plane at 15 GHz, (e) the xoz plane at 17 GHz, and (f) the yoz plane at 17 GHz.

gain bandwidth, and its maxima gain is 25.5 dBi at 15 GHz with 40% aperture efficiency. The measured results agree well with the simulated ones.

Comparison of the proposed wideband FRA with some existing FRAs is shown in Table 2. Obviously, the proposed FRA has the widest 3-dB gain bandwidth and lowest profile. Although the FRAs have higher aperture efficiencies in [3], [14], [15] and [16], their elements have higher profile, which increase the assembly difficulty and processing cost. Moreover, the proposed FRA achieves higher aperture efficiency than the FRAs in [17] and [18] by using only

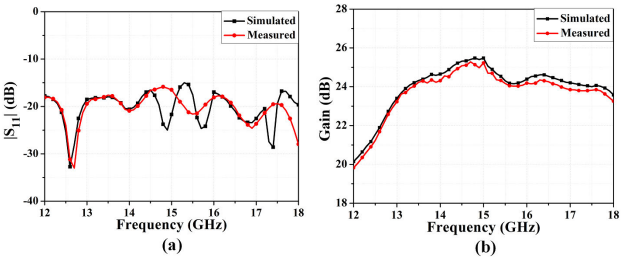

FIGURE 11. Simulated and measured results of the wideband FRA. (a) $|S_{11}|$ and (b) gains.

TABLE 2. Comparison of the proposed antenna with other works.

Ref.	[3]	[14]	[15]	[16]	[17]	[18]	This work
f_0 (GHz)	13	44	10	13	29	29	**15**
Aperture Size	8.6λ	22λ	13.5λ	7.7λ	10.5λ	8.1λ	**9.4λ**
Phase State	Con.	Con.	Con.	Con.	Con.	Con.	**2-Bit**
Height	20.3λ	5.2λ	4.8λ	2.8λ	4.1λ	3.5λ	**2.3λ**
Gain Bandwidth (3-dB)	22.7%	7%	24%	35%	13.2%	37.2%	**39.5%**
Aperture efficiency	50%	49%	44%	49.1%	37%	34.5%	**40%**
Gain	26.7 dBi	31.9 dBi	30 dBi	21 dBi	27.3 dBi	24 dBi	**25.5 dBi**

Note: Con. is continuous

2-Bit phase quantization, which greatly simplifies the design process.

V. CONCLUSION

A novel wideband FRA based on the single-layered polarization rotating metasurface is presented. First, a wideband polarization rotating unit cell consisting of rhombus-shaped metal patch etched on dielectric substrate is designed, which can be used to rotate polarization of the reflective wave 90° relative to that of the incident wave. The element and its mirror image can provide 0°, 90°, 180° and 270° phase shifts with 2-bit phase quantization and more than 80% polarization conversion rates in the Ku band. Due to the introduction of PG and PRM, the distance between the PG surface and the feed phase center can be reduced to about 1/2 of the original focal length. Finally, a wideband FRA is designed, fabricated and measured. The measured results indicate that the proposed reflectarray achieves 39.5% 3-dB gain bandwidth with 25.5 dBi peak gain at 15 GHz. Its maximum aperture efficiency is about 40%. Moreover, its design process is relatively simple, and its processing cost is relatively lower. In particular, the wideband and low-profile features of the proposed FRA make it be easily integrated with other devices and have the potential to be applied to the future communication systems.

REFERENCES

[1] D. Berry, R. Malech, and W. Kennedy, "The reflectarray antenna," *IEEE Trans. Antennas Propag.*, vol. 11, no. 6, pp. 645–651, Nov. 1963.
[2] J. Huang and J. A. Encinar, *Reflectarray Antennas*. Hoboken, NY, USA: Wiley, 2008.

[3] Q.-Y. Chen, S.-W. Qu, X.-Q. Zhang, and M.-Y. Xia, "Low-profile wideband reflectarray by novel elements with linear phase response," *IEEE Antennas Wireless Propag. Lett.*, vol. 11, pp. 1545–1547, 2012.
[4] D. Pilz and W. Menzel, "Folded reflectarray antenna," *Electron. Lett.*, vol. 34, no. 9, pp. 832–833, Apr. 1998.
[5] W. Menzel, D. Pilz, and M. Al-Tikriti, "60 GHz triple folded reflector antenna," *Electron. Lett.*, vol. 38, no. 19, pp. 1075–1076, Sep. 2002.
[6] I.-Y. Tarn, Y.-S. Wang, and S.-J. Chung, "A dual-mode millimeter-wave folded microstrip reflectarray antenna," *IEEE Trans. Antennas Propag.*, vol. 56, no. 6, pp. 1510–1517, Jun. 2008.
[7] B. D. Nguyen, J. Lanteri, J.-Y. Dauvignac, C. Pichot, and C. Migliaccio, "94 GHz folded Fresnel reflector using C-patch elements," *IEEE Trans. Antennas Propag.*, vol. 56, no. 11, pp. 3373–3381, Nov. 2008.
[8] W. Menzel, D. Pilz, and M. Al-Tikriti, "Millimeter-wave folded reflector antennas with high gain, low loss, and low profile," *IEEE Antennas Propag. Mag.*, vol. 44, no. 3, pp. 24–29, Jun. 2002.
[9] A. Zeitler, J. Lanteri, C. Pichot, C. Migliaccio, P. Feil, and W. Menzel, "Folded reflectarrays with shaped beam pattern for foreign object debris detection on runways," *IEEE Trans. Antennas Propag.*, vol. 58, no. 9, pp. 3065–3068, Sep. 2010.
[10] S. Bildik, S. Dieter, C. Fritzsch, W. Menzel, and R. Jakoby, "Reconfigurable folded reflectarray antenna based upon liquid crystal technology," *IEEE Trans. Antennas Propag.*, vol. 63, no. 1, pp. 122–132, Jan. 2015.
[11] J. G. Jeong, N. J. Park, and Y. J. Yoon, "Aperture efficiency improvement of folded reflectarray using rectangle and split-ring combined element," *Electron. Lett.*, vol. 54, no. 13, pp. 797–798, Jun. 2018.
[12] T. P. Nguyen, C. Pichot, C. Migliaccio, and W. Menzel, "Study of folded reflector multibeam antenna with dielectric rods as primary source," *IEEE Antennas Wireless Propag. Lett.*, vol. 8, pp. 786–789, 2009.
[13] X. Y. Lei and Y. J. Cheng, "High-efficiency and high-polarization separation reflectarray element for OAM-folded antenna application," *IEEE Antennas Wireless Propag. Lett.*, vol. 16, pp. 1357–1360, 2017.
[14] J. Ren and W. Menzel, "Dual-frequency folded reflectarray antenna," *IEEE Antennas Wireless Propag. Lett.*, vol. 12, pp. 1216–1219, 2013.
[15] M. Jiang, W. Hong, Y. Zhang, S. Yu, and H. Zhou, "A folded reflectarray antenna with a planar SIW slot array antenna as the primary source," *IEEE Trans. Antennas Propag.*, vol. 62, no. 7, pp. 3575–3583, Jul. 2014.
[16] L. Guo, P.-K. Tan, and T.-H. Chio, "On the use of single-layered subwavelength rectangular patch elements for broadband folded reflectarrays," *IEEE Antennas Wireless Propag. Lett.*, vol. 16, pp. 424–427, 2017.
[17] S.-W. Qu, H.-X. Zhang, W.-W. Wu, P.-F. Li, S. Yang, and Z.-P. Nie, "Wideband folded reflectarray using novel elements with high orthogonal polarization isolation," *IEEE Trans. Antennas Propag.*, vol. 64, no. 7, pp. 3195–3200, Jul. 2016.
[18] X. Liu, Y. Ge, X. Chen, and L. Chen, "Design of folded reflectarray antennas using pancharatnam-berry phase reflectors," *IEEE Access*, vol. 6, pp. 28818–28824, 2018.
[19] Y. Cao, W. Che, W. Yang, C. Fan, and Q. Xue, "Novel wideband polarization rotating metasurface element and its application for wideband folded reflectarray," *IEEE Trans. Antennas Propag.*, vol. 68, no. 3, pp. 2118–2126, Mar. 2020.

WEI SU (Member, IEEE) was born in 1982. He received the B.S. degree from Shandong Agriculture University, Taian, China, in 2005, and the M.S. and Ph.D. degrees from Jinan University, Guangzhou, China, in 2009 and 2013, respectively. His research interests include simulation and test of electromagnetics.

WENHAO LUO was born in 1996. He received the B.S. degree from Jiaying University, Meizhou, China, in 2019. He is currently pursuing the master's degree with the School of Mechanics and Construction Engineering, Jinan University, Guangzhou, China. His research interests include science and technology on reliability physics and application technology of electronic component.

ZHENHUA NIE was born in 1982. He received the B.S. degree from Hebei GEO University, Shijiazhuang, China, in 2006, and the M.S. and Ph.D. degrees from Jinan University, Guangzhou, China, in 2008 and 2012, respectively. His research interests include structural dynamics, structural health monitoring, and artificial intelligence.

WEN-WEN LIU was born in 1981. She received the B.S. and M.S. degrees from the Nanjing University of Science & Technology, Nanjing, China, in 2003 and 2005, respectively, and the Ph.D. degree from Southeast University, China, in 2009. She has been a Research Scientist with the School of Mechanics and Safety Engineering, Zhengzhou University, China, since 2010. Her research interests include modern optical metrology, digital image processing, and antenna design.

ZHEN-HUA CAO was born in 1980. He received the B.Eng. degree from Zhengzhou University, Zhengzhou, China, in 2003, and the M.S. degree from the Nanjing University of Science & Technology, Nanjing, China, in 2005. He is currently with Newcapec Electronics Company Ltd. His research interests include electromagnetic theory, antenna design, electromagnetic compatibility, and product reliability.

ZHI WANG was born in 1981. He received the B.S., M.S., and Ph.D. degrees from Central South University, Changsha, China, in 2004, 2007, and 2010, respectively. He has been a Research Scientist with the School of Mechanics and Safety Engineering, Zhengzhou University, China, since 2010. His research interests include fracture and damage of rock and concrete, antenna design, engineering fatigue problem, and multi-field coupled rock mechanics.